Rare Metal Materials and Engineering
Volume 52, Issue 6, June 2023
Available online at www.rmme.ac.cn

Science Press

Cite this article as: Zhang Jingang, Chen Xing, Li Zhen, et al. Low-Cycle Fatigue Performance and Fracture Mechanism of Nickel-based Single Crystal Superalloy at 530 °C[J]. Rare Metal Materials and Engineering, 2023, 52(06): 1985-1993.

ARTICLE

Low-Cycle Fatigue Performance and Fracture Mechanism of Nickel-based Single Crystal Superalloy at 530 °C

Zhang Jingang[1,2], Chen Xing[1,2], Li Zhen[1,2], Tian Fuzheng[1,2], Liu Xinling[1,2]

[1] Failure Analysis Center of Aero Engine Corporation of China, AECC Beijing Institute of Aeronautical Materials, Beijing 100095, China; [2] Beijing Key Laboratory of Aeronautical Materials Testing and Evaluation, Beijing 100095, China

Abstract: The low-cycle fatigue performance and fracture damage mechanism of Ni-based single crystal superalloy were investigated at 530 °C. Results show that at 530 °C, the fatigue crack of the single crystal superalloy generally appears on the surface, sub-surface or inside of the sample. When there are casting defects on the sub-surface, fatigue crack will arise preferentially from the defects. Under the condition of large strain amplitude (>0.85%), the alloy shows obvious cyclic hardening behavior during the fatigue cycle, and the cyclic stress response curve tends to be stable when the strain amplitude is lower than 0.85%. The plastic deformation of Ni-based single crystal superalloy is mainly proceeded by slip. At 530 °C, the fracture of single crystal superalloy is mainly caused by octahedral slip mechanism, and the main slip system is {111} <110>. According to the sectional structure characteristics of the fracture, no obvious plastic deformation occurs near the source area. The characteristic of fatigue striation can be seen in the stable extension of the crack, and a lot of cross slip bands exist at the slip step in the rapid crack extension stage. By electron backscattered diffraction analysis, there are obvious plastic deformation on the fracture surface at the junction of different slip planes, and the γ matrix and cubic γ' phase near the fracture surface are seriously distorted. No obvious oxidation is observed on the surface of fatigue fracture at 530 °C .

Key words: single crystal superalloy; low cycle fatigue; octahedral slip; cyclic hardening

Nickel-based single crystal superalloy has been widely used in the hot section components of aero-engines due to its excellent properties such as high temperature creep resistance, thermal mechanical fatigue resistance and oxidation corrosion resistance[1–3]. As the key hot section material of aero-engine, turbine blades are prone to failure due to long-term service in extreme environment such as complex temperature field and stress field, thus affecting the overall performance of aero-engine. According to statistics, the main failure mode of the turbine blade is fatigue fracture[4–7]. Due to the complex geometry of turbine blades, the temperature and stress of blades in different parts differ greatly in actual service, and the coupling effect of high temperature and vibration generally leads to high-cycle fatigue in the body of turbine blade [8–10]. Although the service temperature of the tenon part of turbine blade is lower than the blade body, it is prone to low-cycle fatigue failure due to the effect of centrifugal force. Cao et al[11] studied the low-cycle fatigue behavior of single crystal superalloy at 760 and 980 °C, and found that the cyclic hardening degree of the material is better at low temperature, while the fatigue performance is deteriorated at high temperature. Zhang et al[12] studied the low-cycle fatigue behavior of single crystal superalloy under different strain ratios at 1100 °C and revealed that the cyclic softening or hardening behavior of the material is related to the microstructure and loading state of the alloy.

At present, most of the research focuses on the medium and high temperature low-cycle fatigue performance of single crystal superalloy. For the tenon part of the turbine blade, whose service temperature is generally lower than 760 °C[13], low-cycle fatigue failure is prone to generate. According to a large number of failure cases, the actual service temperature of the tenon is about 530 °C. At present, there is no research report on low-cycle fatigue of single crystal superalloy at

Received date: December 27, 2022
Foundation item: National Science and Technology Major Project (J2019-VI-0022-0138)
Corresponding author: Liu Xinling, Ph. D., Professor, AECC Beijing Institute of Aeronautical Materials, Beijing 100095, P. R. China, Tel: 0086-10-62496239, E-mail: liuxinling119@163.com

530 °C. In this work, the temperature of 530 °C was selected to simulate the service temperature of the tenon part of the turbine blade. By analyzing the fracture characteristics and microstructure evolution of the single crystal superalloy in different fatigue cycles, the low-cycle fatigue damage behavior and fracture mechanism of the single crystal superalloy were revealed.

1 Experiment

The material used in the test was the second generation nickel-based single crystal superalloy developed by Beijing Institute of Aeronautical Materials. The nominal composition of the alloy is shown in Table 1. The cylinders of single crystal superalloy with [001] orientation were prepared by spiral crystal separation in a vacuum directional solidification furnace with high temperature gradient. The orientation of the test bar deviating from [001] was within 15°, which was determined by X-ray backscattering method. As-cast specimens were heat treated at 1290 °C for 1 h, 1300 °C for 2 h, 1315 °C for 4 h, and then aged at 1120 °C for 4 h and 870 °C for 32 h, both followed by air cooling. The matrix microstructure after heat treatment is shown in Fig.1.

After heat treatment, the specimens were processed into standard fatigue samples (M2504-S089) according to the Atlas of Metal Mechanical Property Samples (Q/6S 977-2004). The low-cycle fatigue test was conducted by the MTS servo hydraulic testing machine and the sample was heated by the resistance furnace at 530 °C. Total strain-range-control was adopted in the test, the strain ratio was 0.05, and stress waveform was triangular. After the fatigue test, the fatigue fracture surfaces were observed by stereoscopic microscope (Leca) and field emission scanning electron microscope (Gemini SEM300) after cleaning. Wire cutting technology was used to cut the fracture surface longitudinally along the source region. The longitudinal section of the fracture was mechanically polished, followed by vibration polishing for 8 h. The plastic deformation near the fracture surface was analyzed by back scattering diffraction (EBSD). The change of microstructures near the fracture surface was examined after etching with 5 mL H_2SO_4+3 mL HNO_3+92 mL HCl.

Table 1 Nominal compositions of single crystal superalloy (wt%)

Cr	Co	W	Mo	Al	Ta	Re	Hf	Nb	Ti	Ni
4	9	8	2	6	7	2	0.2	1.0	0.1	Bal.

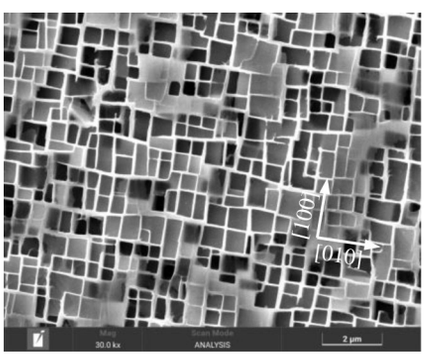

Fig.1 Microstructure of nickel-based single crystal superalloy after heat treatment

2 Results and Discussion

2.1 Low cycle fatigue performance

For the low cycle fatigue test, total strain-range-control was adopted and the strain ratio was 0.05 at 530 °C. The relationship between fatigue cyclic life and strain amplitudes is shown in Fig. 2a. With the decrease in strain amplitude, the fatigue cyclic life of single crystal superalloy increases gradually. At the $\Delta\varepsilon/2$ values of 0.5%, the fatigue cyclic life of the alloy reaches 1×10^4. It has been reported that the fatigue cyclic life of single crystal superalloy can reach 1×10^4 when the strain amplitude is about 0.7% at 760 °C[14]. It can be seen that temperature has a great influence on the low cycle fatigue performance of single crystal superalloy. With the increase in strain amplitude, the stress amplitude of low-cycle fatigue test of single crystal superalloy gradually increases, as shown in Fig. 2b. When the strain amplitude is about 0.5%, the stress amplitude $\Delta\sigma/2$ of the alloy reaches 600 MPa. The stress amplitude $\Delta\sigma/2$ of the alloy is more than 1000 MPa when $\Delta\varepsilon/2$ is about 1%. Compared with the high cycle fatigue test, the nominal stress of single crystal superalloy in low cycle fatigue test is larger[15].

In the process of low-cycle fatigue test, real-time monitoring was carried out for each given strain amplitude test to record the change of test stress with the number of cycles. Fig. 3 shows the variation curve of the peak cyclic stress of single crystal superalloy with the fatigue cycles under

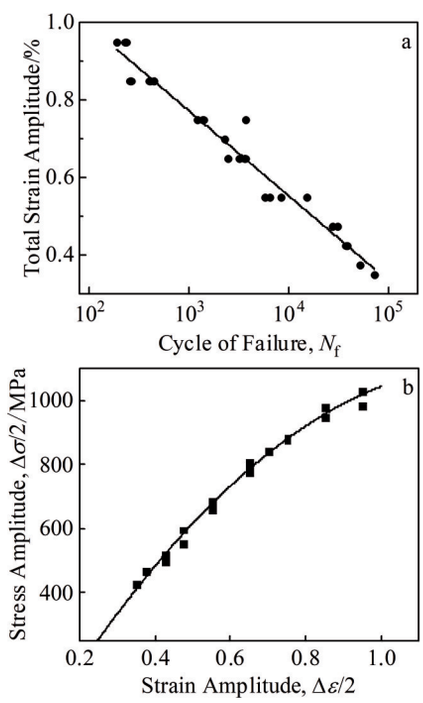

Fig.2 Low cycle fatigue performance of single crystal superalloy at 530 °C: (a) relationship between fatigue cycle life and strain amplitude; (b) stress-strain curve

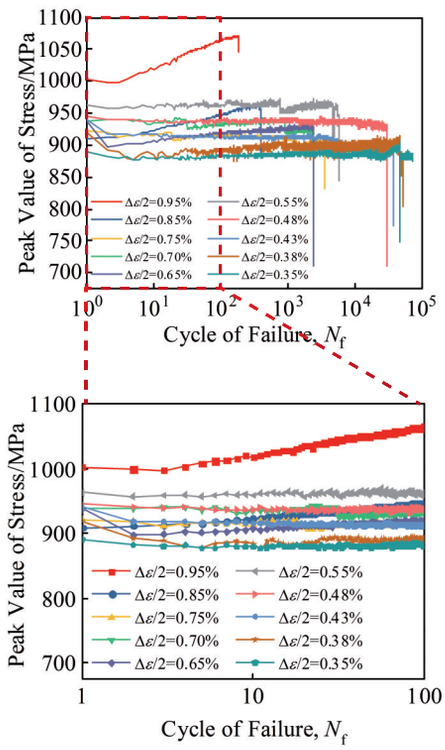

Fig.3 Cyclic stress response curves of the alloy at different strain amplitudes and 530 °C

different strain amplitudes at 530 °C. As can be seen from the curve, when the strain amplitudes are 0.95% and 0.85%, the peak value of cyclic stress gradually increases with the increase in the fatigue cycles. Meanwhile, the alloy shows the characteristics of cyclic hardening. When the strain amplitudes are 0.65%, 0.43% and 0.38%, there is a slight cyclic softening behavior at the initial stage of the cycle. The cyclic stress response curve tends to be stable for the residual strain amplitude.

Cyclic hardening/softening is directly related to the motion of the dislocation. For cyclic hardening, dislocation diffuses in the γ channel due to the effect of external stress. At the same time, the motion of the dislocation in the γ channel is hindered by the cubic γ' phase, which induces a large number of dislocations in the blockage and requires further stress to move the dislocation. Cyclic softening is caused by the merging and rearrangement of dislocations to restore the alloy. In addition, dislocation intrusion into the γ' phase can also lead to cyclic softening. The stress stabilization stage is the result of the interaction between cyclic hardening and cyclic softening to achieve dynamic equilibrium.

The cyclic hardening behavior of single crystal superalloy only occurs in large strain stage at 530 °C. As reported in Ref. [16], the single crystal superalloy undergoes cyclic softening first and then cyclic hardening at 800 °C. On the contrary, it shows cyclic hardening first and then cyclic softening at 980 °C.

2.2 Fracture characteristics

The fatigue fracture of single crystal superalloy can be generally divided by three stages: fatigue source stage, fatigue crack propagation stage and instantaneous fracture stage. The fatigue crack growth stage can be divided into stable crack growth zone and fast crack growth zone. At 530 °C, the fatigue fracture of single crystal superalloy generally starts from the surface, sub-surface or inside of the sample.

Fig. 4 shows the fracture morphology with fatigue crack initiation characteristic on the surface. The fatigue fracture is shear fracture, and the angle between the fracture plane and the axial force is 36°. The morphology near the source region

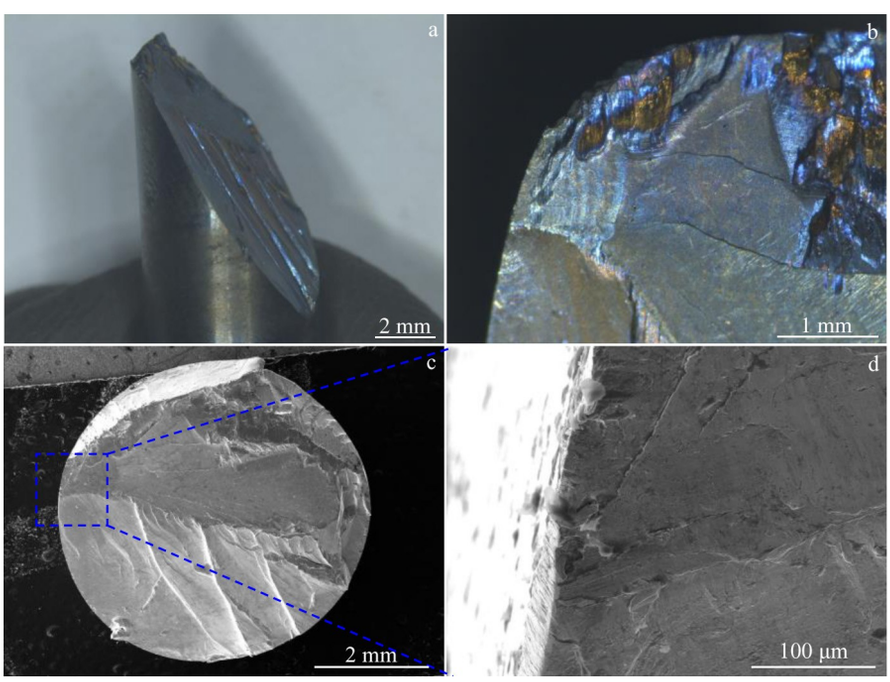

Fig.4 Fatigue crack initiation on the specimen surface (Δε/2=0.95%)

is flat, no abnormalities are found on the sub-surface, and the characteristics of fatigue striation can be seen in the steady crack growth stage as shown in Fig.4b. The expanded ridge on the fatigue fracture surface is distributed in fluvial pattern.

As shown in Fig. 5, the fracture originates from the internal of the specimen. Obvious secondary cracks exist near the source region in Fig. 5d. The fatigue cracks propagate along two different {111} slip planes after initiation in the interior of the alloy. Obvious fatigue striation can be seen in the steady crack growth stage from Fig. 5b. Due to the long-term high temperature environment on the fracture surface during the crack initiation and steady growth stage, the color of the fatigue fracture surface at this stage is bluish violet, which is obviously different from the normal temperature metallic color in the instantaneous fracture stage. Thus, for the low-cycle fatigue fracture surface of single crystal superalloy, the main fatigue life is consumed in the fatigue crack initiation and stable growth stage.

As can be seen from Fig. 6, the fatigue crack usually originates from the casting defects when casting defects exist on the sub-surface. Due to the stress concentration in casting defect, fatigue cracks are prone to accumulate in casting defect under the action of greater stress. In the case of large strain and low cyclic life ($\Delta\varepsilon/2$= 0.85%, N_f=398), as shown in Fig.6a–6c, the crack originates from casting defect of the sub-surface and then propagates along the specific octahedral slip plane until fracture. The fatigue fracture surface is an inclined shear surface. There are characteristics of abrasion and extrusion on the fracture surface, and obvious slip bands feature in the rapid crack propagation stage. When the strain amplitude is 0.7%, the crack originates at more than one casting defect, and the fatigue fracture is composed of two different {111} slip planes. A large number of cross-slip characteristics exist at the junction of the crack in the stable growth stage and the rapid growth stage (Fig. 6f). When the strain amplitude is 0.48%, the location of the casting defect where the fatigue source area is located is far away from the surface, and the fatigue area of the stable crack growth stage increases. The characteristics of fatigue striation are obvious on the fracture surface, and the spacing between fatigue striation is obviously narrower than that of the fracture with large strain amplitude (Fig. 6i). As a whole, the initiation location and critical crack length of low-cycle fatigue fracture change regularly with the decrease in strain amplitude.

For metallic materials, the slip usually occurs along the densely packed plane and the densely packed direction. Nickel-based single crystal superalloy is face-centered cubic structure, and the octahedron and cubic hexahedron are high-density atomic arrangement planes. Therefore, octahedral and cubic hexahedral plane slips are the main deformation mechanism of nickel-based single crystal superalloy. According to Ref. [17], for nickel-based single crystal superalloys, the octahedral slip system is mainly operated below 900 °C, and the octahedral slip system and the cubic hexahedral slip system are operated at the same time above 900 °C. Under 900 °C, the fatigue fracture of nickel-based single crystal superalloys generally presents one or more inclined planes. This inclined plane is exactly the {111} crystal plane of the atomic close-packed plane from the perspective of crystallography. Because the connection between the {111} crystal planes is relatively thin and weak, slip generally occurs here when plastic deformation occurs in face-centered cubic metal. When the temperature is higher than 900 °C[18], the fracture is generally quasi-plane on the macro level, the fracture plane direction is basically perpendicular to the axial force direction, and small part of the fracture has an inclined

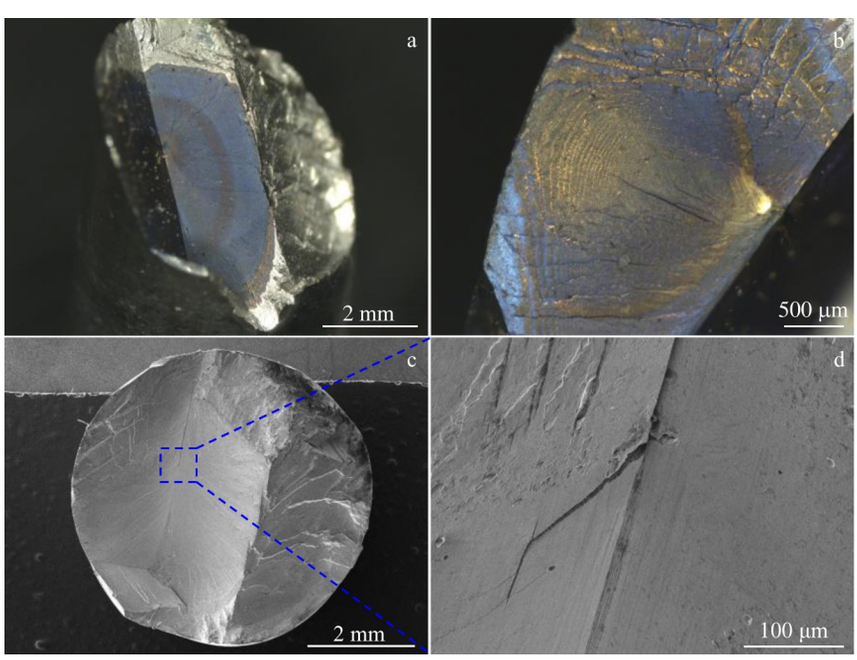

Fig.5 Fatigue crack initiation in the internal of the specimen ($\Delta\varepsilon/2$=0.5%)

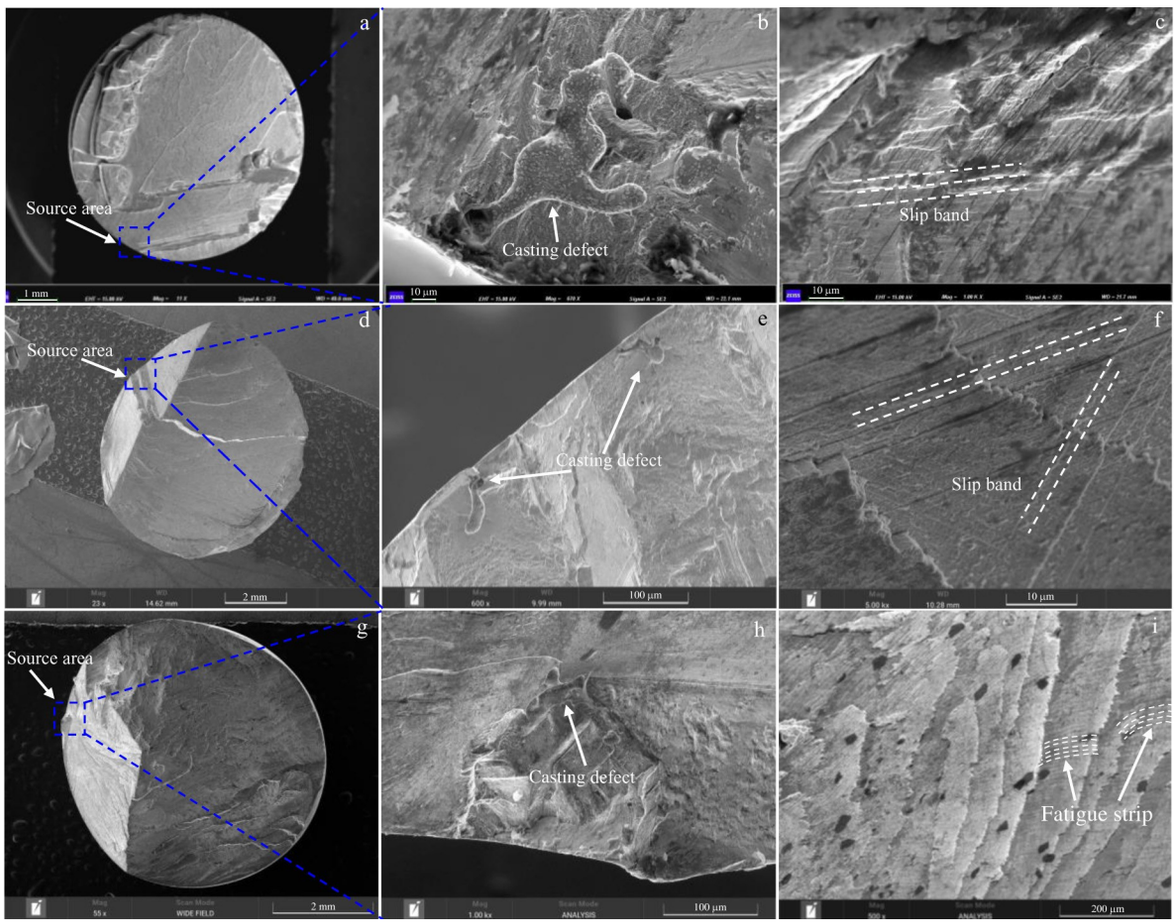

Fig.6 Fatigue cracks initiated at the casting defects of the sub-surface: (a–c) $\Delta\varepsilon/2$=0.85%, (d–f) $\Delta\varepsilon/2$=0.7%, and (g–i) $\Delta\varepsilon/2$=0.48%

plane in the shear lip area, so the octahedral slip and cubic hexahedral slip generally occur at the same time above 900 °C.

Low-cycle fatigue tests were carried out at 530 ° C. According to the origin of fatigue fracture and the crack growth path, the deformation mechanism at 530 ° C is mainly octahedral slip, with the main slip system of {111}<110> and the secondary slip system of {111}<112>. When the strain amplitude is large, the fatigue cracks are easy to originate from the surface and sub-surface. In addition, the fatigue crack usually originates from the casting defects when it exists on the sub-surface. When the fatigue life is low, the crack grows rapidly along the {111} slip plane at a certain angle to the axial direction, which is easy to form a single shear plane, and extrusion marks exist on the fracture surface. With the increase in fatigue life, the crack can propagate along different {111} slip planes, and the fatigue fracture has two or more shear planes. For the fracture with casting defects, with the increase in fatigue life, the location of casting defects starts to be far away from the surface.

Fig. 7 shows the corresponding fracture morphologies at different stages in the process of fatigue crack growth. At the stage of crack stable growth, the fracture surface is characterized by fluvial pattern expanded ridge and fatigue striation. The expanded ridge is perpendicular to the fatigue striation and consistent with the direction of crack growth. It is found that the expanded ridge is actually a small tear slip surface when observed with a high magnification microscope. Due to the height difference between the small slip surface and the fracture surface, it presents the ridge feature at low magnification (Fig. 7a). The microstructure of the stable crack growth stage shows clear characteristics of γ channel and γ' phase in Fig. 7b. Although the color of the fatigue area is bluish violet at 530 ° C, the oxidation degree of the fracture surface is weak and no obvious oxidation products are found.

A large number of parallel and cross slip bands exist at the junction of the crack at the stable and rapid growth stages. The plastic deformation near the fracture surface increases with the acceleration of the crack growth rate at the rapid growth stage. Meanwhile, the slip bands quickly converge and are distributed among a large number of small slip planes, forming slip steps (Fig. 7d). With the increase in crack growth rate, the spacing of the slip step gradually increases. At the final fracture stage, the cracks rapidly expand along one of the slip planes to the entire fracture. As shown in Fig. 7f, the fracture of the slip plane is the unique tear dimple morphology of single crystal superalloy.

2.3 Micromorphology of fatigue fracture section

In the process of low-cycle fatigue crack propagation, the crack tip opens and closes with the action of alternating load, which promotes the crack propagation. The deformation of

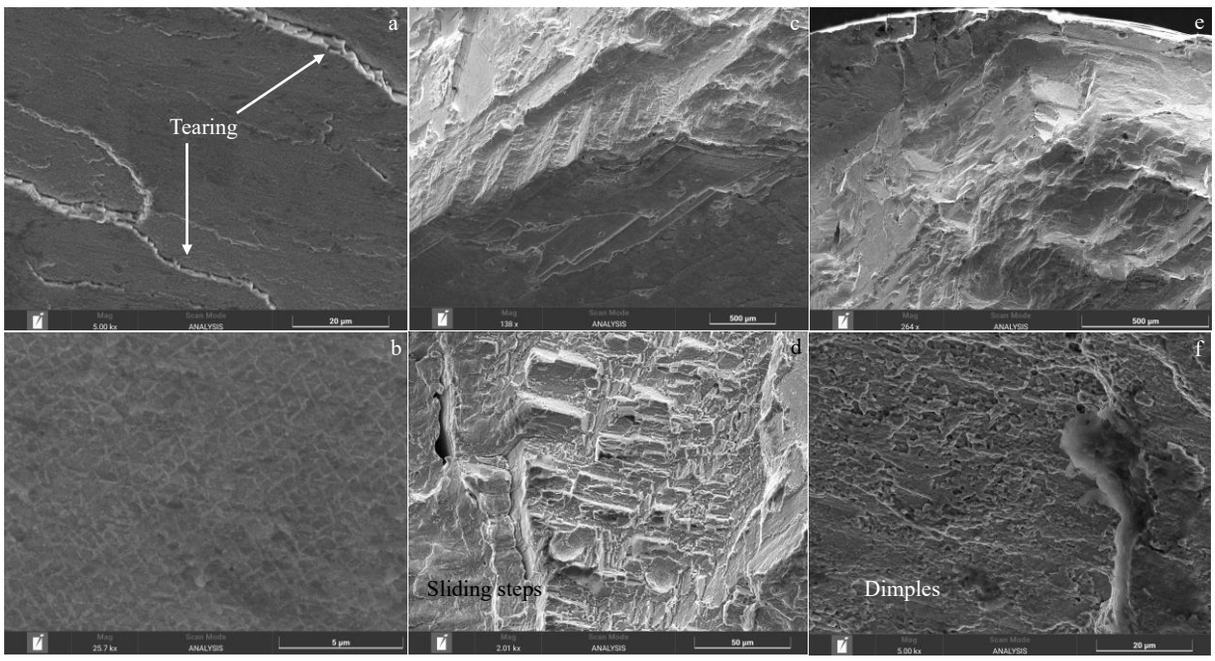

Fig.7 Fracture morphologies of crack at stable crack growth stage (a – b), slip steps during rapid crack growth stage (c – d) and dimple morphologies in instantaneous fracture stage (e–f)

single crystal superalloy is mainly slip. Therefore, the mechanism of fatigue crack propagation can be analyzed by studying the slip behavior of fatigue fracture.

For the sample with strain amplitude of 0.7%, the longitudinal section of the fracture is obtained by longitudinal cutting along the crack growth direction near the source region, as shown in Fig.8a. After chemical corrosion, the cross section microstructure near the fatigue fracture is observed. The structure of γ matrix and cubic γ' phase near the fatigue source is intact. No obvious plastic deformation and oxide layer are found on the fracture surface. There is no secondary crack on the outer surface of the sample (Fig. 8b), which is obviously different from the fatigue behavior of single crystal superalloy at high temperature. According to Ref. [19 – 21], oxidation at high temperature will promote the generation of cracks on the surface of the sample, and then a large number of small vertical axial cracks occur on the outer surface of the sample. It can be concluded that the temperature has little effect on fatigue crack growth at 530 ° C, and material properties and applied force are the main influencing factors.

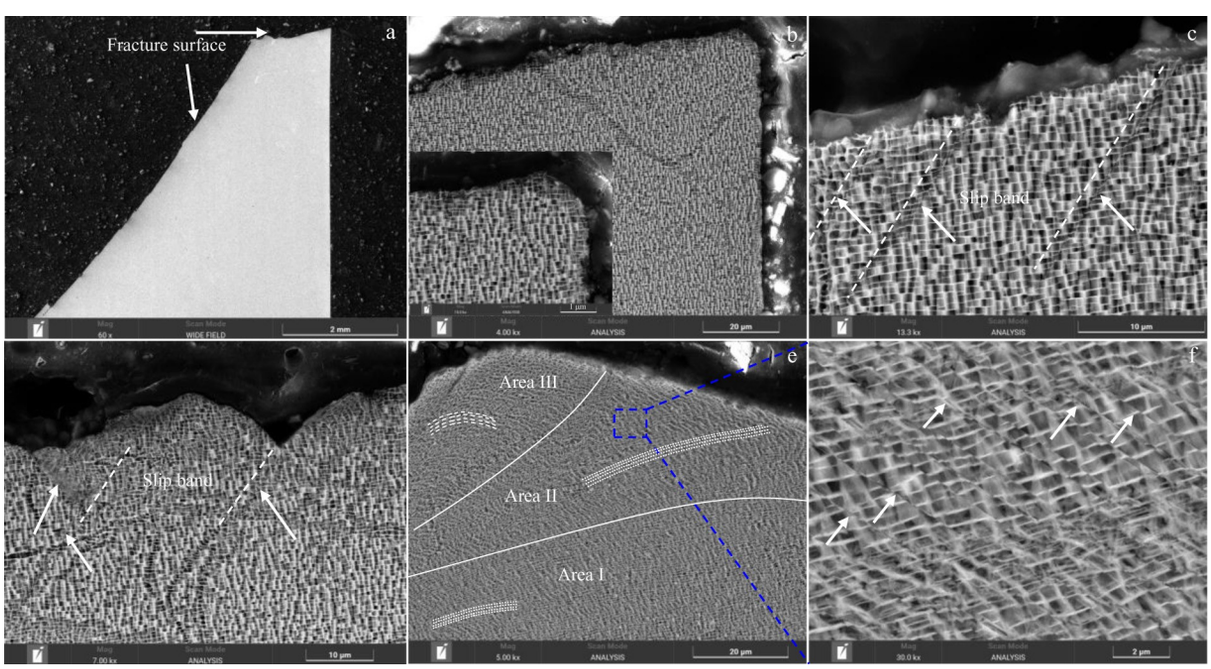

Fig.8 Microstructures of fatigue fracture section along the direction of crack propagation ($\Delta\varepsilon/2$=0.7%)

When the crack continues to expand to a little distance from the fatigue source region, a few parallel slip lines appear near the fracture surface, as indicated by the white arrow in Fig.8c. The slip line tilts at a certain angle to the fracture surface, and the γ matrix and γ' phase near the slip line are deformed; the cubic frame of γ matrix is interrupted, and the phenomenon of intrusion and extrusion caused by slip exists on the fracture surface. As the fatigue crack further expands to the slip step, obvious plastic deformation can be seen on the surface of the fracture (Fig. 8d). The number of slip lines increases and the directions are inconsistent. The slip lines intersect each other to form cross slip bands. When the fatigue crack extends to the junction of two different {111} slip planes, as shown in Fig. 8e, the plastic deformation of the fracture surface is serious. According to the deformation direction of γ matrix and cubic γ' phase (the white dotted line), the area near the fracture surface at the junction can be divided into three deformation zones. The deformation direction of γ matrix and γ' phase in different regions is roughly consistent with the direction of fatigue crack growth. It can be seen from the microscopic morphology in Fig. 8f that the γ matrix and γ' phase are cut by a large number of slip bands, and the γ matrix and γ' phase are inclined along the crack propagation direction under the action of force. From Fig. 8e, the γ matrix and γ' phase near the fracture surface have a larger inclined angle along the crack growth direction, while the matrix structure inside the sample has a smaller inclined angle. When the inclination angle of γ matrix and γ' phase reaches a certain degree and the crack tip exerts alternating load continuously, the fatigue crack gradually transits from the initial {111} slip plane to another one. Therefore, the fracture of low-cycle fatigue usually has two or more octahedral slip planes.

Due to the rapid crack propagation rate in the instantaneous fracture stage, the feature of tear dimple appears on the fracture surface, and some fractures have the appearance of wear extrusion in the instantaneous fracture stage. Fig. 9 shows the microstructure of the cross section of the wear extrusion in instantaneous fracture zone. A serious distortion layer on the fracture surface in this area, and the γ matrix and γ' phase in the distorted region are extruded into layered characteristics. A large number of secondary cracks exist in the distorted layer, and there are slip bands parallel to the fracture surface on the sub-surface of the fracture.

2.4 Electron backscattering diffraction analysis

Electron backscattering diffraction (EBSD) technique can be used to analyze the crystal structure and orientation of materials. Although there is no grain boundary of single crystal superalloy, the matrix structure is composed of γ matrix and cubic γ' phase. During the low-cycle fatigue test, the matrix structure near the crack tip is prone to deformation under the action of alternating load. EBSD technology can express the plastic deformation behavior more directly by calculating the orientation change of microstructures.

Fig. 10 shows the plastic deformation information of fracture surface at the junction of two different octahedral slip planes. The crack propagates from slip plane I to slip plane II. From the IPF diagram (Fig. 10b), the axial crystal orientation of the sample is in the direction of [001]. When the fatigue crack extends to the end of slip plane I, the crystal orientation of the structure near the fracture surface changes from [001] to [111] or [101], and no recrystallization morphology is observed on the fracture surface. The crystal orientation of the sub-surface changes from [001] to the orientation between [001] and [111]. When the fatigue crack extends to slip plane II, the crystal orientation on the fracture surface does not change significantly. Fig. 10c is the KAM (kernel average misorientation) diagram of the fracture surface of the sample, and the color variation area of the fracture surface represents the plastic deformation area. It can be seen that there is serious plastic deformation on the fracture surface during the transition of slip surface, which corresponds to the distortion morphology of γ matrix and γ' phase as shown in Fig.8e.

KAM diagram is the most commonly used method for the analysis of local misorientation, which is generally used to analyze the local strain distribution of crystal materials. In addition, KAM diagram can also be used to calculate the geometric dislocation density in crystal materials. In the KAM diagram, the KAM value of each data point is the average of the misorientation between all other data points and the data point in the center within a certain radius. Therefore, the change of dislocation density and strain in this region can be judged according to the change of KAM value.

Based on Fig. 10c, Fig. 11 shows the change of kernel average misorientation along the fracture surface to the inside of the sample. In order to make the test data accurate, three different positions were taken for measurement. The results

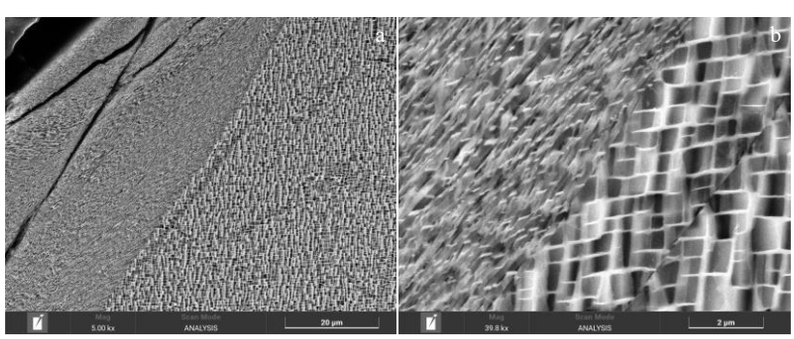

Fig.9 Microstructures of cross section of the wear extrusion in instantaneous fracture zone ($\Delta\varepsilon/2$=0.7%)

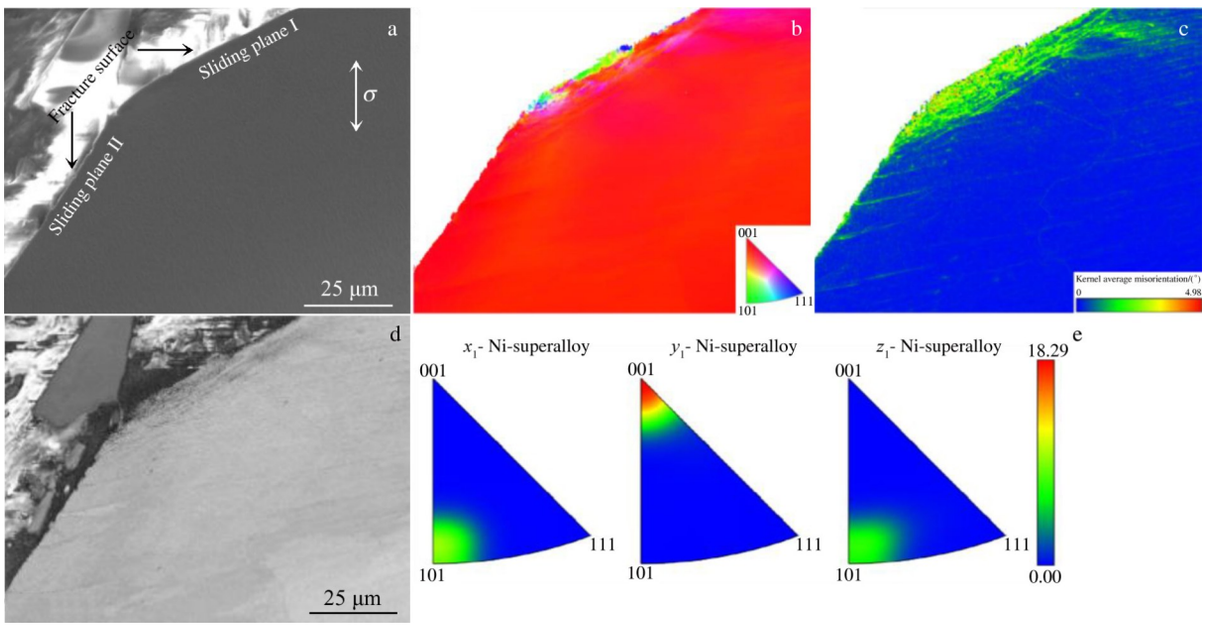

Fig.10 Plastic deformation at the junction of two slip surfaces analyzed by EBSD

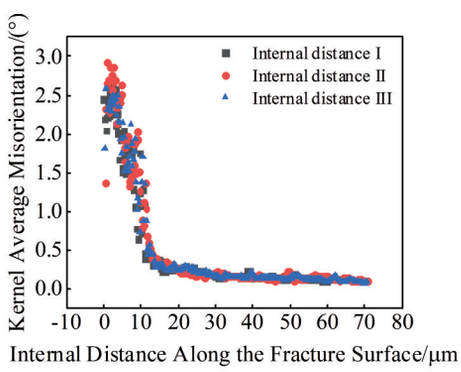

Fig.11 Change of kernel average misorientation from the fracture surface to the inside of the sample

show that the value change of kernel average misorientation starts to flatten out at about 18.49 μm inward along the fracture surface. Therefore, 18.49 μm can be used to represent the size of plastic deformation zone on the fracture surface.

2.5 Parameter analysis of fatigue fracture surface

Table 2 shows the extraction information from the surface of the fatigue fracture. Among them, the angle between the fatigue surface and the axial force direction and the length of critical crack propagation are included. The size of the fatigue source area and the distance from the source area to the surface were extracted for the sample with casting defects. By analyzing the quantitative information of the fracture surface, it is found that the angle between the fatigue surface and the axial force is approximately 40°, which is consistent with the octahedral slip mechanism of face-centered cubic metals. However, its relationship with fatigue cyclic life is not clear. The length of critical crack tends to increase with the increase in fatigue life. For the fatigue fracture with casting defects, the area of the casting defects decreases with the increase in fatigue cyclic life, and the distance between the defects and the surface increases with the increase in fatigue cyclic life.

By studying the influence of three different parameters, including the length of critical crack a_c, the area of defect in the fatigue source region S, and the distance from the source region to the surface d, on the fatigue cyclic life, and fitting the existing data, the relationship between the three parameters and the fatigue cyclic life is as follows:

Table 2 Extracted information from the surface of the fatigue fracture

Sample No.	$\Delta\varepsilon/2$	N_f	Source type	Source position	Source size/μm	d/μm	Crack angle/(°)	a_c/mm
530-01#	0.95	188	-	Surface	-	-	36	1.71
530-02#	0.75	3645	Defects	Sub-surface	26	8	42	1.86
530-03#	0.7	2256	Defects	Sub-surface	123	10	39	2.24
530-04#	0.65	2476	Defects	Sub-surface	43	12	45	2.28
530-05#	0.55	5716	-	Sub-Surface	-	-	40	2.52
530-06#	0.5	27854	Crack	Interior	-	-	43	2.87
530-07#	0.48	30616	Defects	Sub-surface	75	132	38	2.81
530-08#	0.43	37741	Defects	Sub-surface	66	138	42	2.47
530-09#	0.35	73761	Defects	Sub-surface	68	440	36	3.34

$\lg N_f=0.3515\ \lg[(a_c d^2)/S]+1.8804$

For the low-cycle fatigue fracture of single crystal superalloy, the relationship between fracture parameters and fatigue life can be established according to the known information extracted from the fracture surface, such as $\lg N_f = A\ \lg[(a_c d^2)/S] + B$. For the same material, low-cycle fatigue life can be predicted according to the above model.

3 Conclusions

1) At large strain amplitudes of 0.95% and 0.85%, the nickel-based single crystal superalloy shows cyclic hardening during the fatigue cycle. When the strain amplitude is lower than 0.85%, the cyclic softening behavior only appears in the early stage, and then the cyclic stress response curve tends to be stable.

2) Under the condition of 530 °C and strain ratio of 0.05, the low-cycle fatigue cracks of single crystal superalloys generally initiate on the surface, sub-surface or interior of the specimen. Most of the fatigue cracks originate from the casting defects of sub-surface. Slip is the main deformation mechanism of single crystal superalloy. At 530 °C, the alloy is mainly fractured by octahedral slip mechanism and the main slip system is {111}<110>.

3) No obvious plastic deformation can be found near the fatigue source area. A lot of cross slip bands at the slip step in the rapid crack growth stage and the γ matrix and cubic γ' phase near the surface have serious deformation. Obvious plastic deformation exists on the fracture surface at the junction of different slip planes, and no oxidation is observed on the fracture surface.

References

1 Bing Z, Xin L, Liu D *et al*. *Materials Science & Engineering A*[J], 2012, 551: 149

2 Tan X P, Liu J L, Jin T *et al*. *Materials Science and Engineering A*[J], 2013, 580(10): 21

3 Wen Z, Zhang D, Li S *et al*. *Journal of Alloys and Compounds*[J], 2017, 692: 301

4 Shi Z X, Wang X G, Liu S Z *et al*. *Progress in Natural Science: Materials International*[J], 2015, 25(1): 78

5 Xie Hongji, Li Jiarong, Han Mei *et al*. *Rare Metal Materials & Engineering*[J], 2018, 47(8): 6 (in Chinese)

6 Hu Chunyan, Liu Xinling, Tao Chunhu *et al*. *Failure Analysis and Prevention*[J], 2014, 9(4): 5 (in Chinese)

7 Li S, Ping L. *Rare Metal Materials & Engineering*[J], 2015, 44(2): 288

8 Shui L, Jin T, Sun X *et al. International Journal of Modern Physics B*[J], 2010, 24: 2886

9 Xie H J, Li J R, Yue X D *et al*. *Materials Science Forum*[J], 2017, 898(1): 480

10 Yu J J, Sun Y L, Sun X F *et al. Materials Science & Engineering A*[J], 2013, 566: 90

11 Cao Gang, Zhang Xuhui, Xu Tao *et al. Hot Working Technology*[J], 2017(22): 4 (in Chinese)

12 Zhang Shichao, Li Xudong, Yu Huichen *et al. Journal of Aeronautical Materials*[J], 2018, 38: 95 (in Chinese)

13 Liu Weiwei, Tang Dingzhong, Li Jiarong *et al. Journal of Aeronautical Materials*[J], 2012, 32: 2 (in Chinese)

14 Shi Zhenxue, Li Jiarong, Liu Shizhong *et al. Transactions of Materials and Heat Treatment*[J], 2011, 32(5): 41 (in Chinese)

15 Shi Z X, Li J R, Liu S Z *et al*. *Transactions of Nonferrous Metals Society of China*[J], 2011, 21(5): 998

16 Shi Z X, Hu Y T, Liu S Z *et al*. *Materials for Mechanical Engineering*[J], 2021, 45(3): 16

17 Ding Z P, Liu Y L, Yi Z Y *et al*. *Journal of Mechanical Strength*[J], 2003, 25(3): 254

18 Liu L, Jie M, Liu J L *et al. Acta Metallurgica Sinica*[J], 2019, 32: 381

19 Chen B, Zhao Z, Zhang F *et al*. *Metallurgical and Materials Transactions A*[J], 2020, 51(4): 1

20 Zhao Z, Li Q, Zhang F *et al*. *International Journal of Fatigue*[J], 2021,150: 106 343

21 Zhao Z, Liang Z, Li Q *et al*. *Materials Science and Engineering A*[J], 2022, 836: 142 711

镍基单晶高温合金530 ℃低周疲劳性能及断裂机制

张金刚[1,2]，陈　星[1,2]，李　振[1,2]，田福政[1,2]，刘新灵[1,2]

(1. 中国航发北京航空材料研究院 中国航发失效分析中心，北京 100095)

(2. 航空材料检测与评价北京市重点实验室，北京 100095)

摘　要：对镍基单晶高温合金在530 ℃的低周疲劳断口及断裂损伤机制进行研究。结果表明：在530 ℃时，单晶高温合金低周疲劳裂纹一般萌生于试样表面、亚表面或内部。亚表面存在铸造缺陷时裂纹从缺陷处起源。在大应变幅（>0.85%）条件下，合金在疲劳循环过程中表现出明显的循环硬化行为，应变幅低于0.85%时循环应力响应曲线基本趋于稳定。镍基单晶高温合金主要通过滑移产生变形，在530 ℃合金主要通过八面体滑移机制进行断裂，主滑移系为{111}<110>。分析断口特征可知，断口在源区附近未见明显塑性变形，稳定扩展区可见疲劳条带特征，快速扩展区在滑移台阶处存在大量交叉滑移带。通过电子背散射衍射分析发现，不同滑移面交界处的断口表面存在明显塑性变形，靠近断口表面的γ基体及立方γ'相变形严重。该温度下疲劳断口表面未见明显氧化特征。

关键词：单晶高温合金；低周疲劳；八面体滑移；循环硬化

作者简介：张金刚，男，1995年生，博士，中国航发北京航空材料研究院，北京 100095，电话：010-62496136，E-mail：jingangpri@163.com